International Journal of Energy and Sustainable Development
Vol. 3, No. 1, 2018, pp. 8-28
http://www.aiscience.org/journal/ijesd

Techno-Economic and Environmental Impact Analysis of a Combined Cycle Power Plant with Internal Cooling of Inlet Air Streams to the Compressor and Condenser

Ifeanyi Henry Njoku*, Chika Oko, Joseph Ofodu

Department of Mechanical Engineering, Faculty of Engineering, University of Port Harcourt, Choba, Port Harcourt, Nigeria

Abstract

This paper presents the thermodynamic, economic and environmental impact assessment of an existing combined cycle power plant to be retrofitted with a waste heat driven aqua lithium bromide absorption refrigerator for cooling the inlet air streams to the compressor and air cooled steam condenser. The power plant is located in the hot and humid tropical region of Nigeria, latitude 4°45′N and longitude 7°00′E. Using the operating data of the plant, the results of the analysis showed that by cooling the inlet air to the compressors to 15°C, the net power output of the gas turbine cycles increased by 48.3MW, and by cooling the inlet air streams to the air cooled steam condenser to 29°C, the net power output of the steam turbine cycle increased by 1.4MW. The overall thermal efficiency of the plant increased by 8.1% while the specific fuel consumption decreased by 7.0%. The stack flue gas exit temperature reduced from 126°C to 84°C in the absorption refrigerator, thus reducing the exhaust heat discharge rate to the atmosphere. The total capital cost, life cycle cost, annual sales revenue and net present value increased by 3.3%, 2.3%, 7.7% and 17%, respectively while the levelized cost of energy production in the plant and the break-even point of the investment reduced by 4.8% and 5.6%, respectively. Environmental impact analysis revealed that the emission rates of NOx and CO_2 emissions per MWh decreased by 65% and 7.3% respectively while the rate of CO emission increased with inlet air cooling by 12.1%. Thus inlet air cooling offers improved thermodynamic output, increased return on investment and greater environmental sustainability.

Keywords

Absorption Refrigeration, Combined Cycle Power Plant, Techno-economic Analysis, Environmental Impact Analysis, Psychrometric Processes, Waste Heat Utilization

Received: February 4, 2018 / Accepted: March 10, 2018 / Published online: April 9, 2018

1. Introduction

Sustainable power generation requires continuous power plant efficiency improvement. The combined cycle power plant technology has become very attractive for electric power production (fossil fuel-to-electric energy conversion) due to its comparatively high efficiency and lower environmental impact than the single cycle power plant [1]–[3]. However, in a CCPP the power capability is significantly affected by the ambient temperature [4]. For a combined cycle power plant operating with air cooled condenser, the ambient air conditions have direct impact on the performance of both the gas- and steam-turbine cycles, respectively [5]. The gas turbine is designed to operate with a constant air volume flow in the compressor and normally at inlet air temperature of 15°C ISO condition [6]. When the inlet ambient air temperature increases, its specific volume increases, so that the mass flow rate entering the turbine is accordingly decreased, leading to decrease in the power

* Corresponding author
E-mail address: njokuhi@gmail.com (I. H. Njoku)

output of the gas turbine [7]. Thus, the power output is dependent on the mass flow rate of the air in the plant. For each degree Celsius increase of the air temperature, the power outputs of the gas turbine and the combined cycles are reduced by 0.5–0.9% and 0.27%, respectively [8].

The performance and power output of the gas turbine power plant strongly depend on the compressor inlet air temperature [11,12]. Different inlet air cooling technologies are available for improving gas turbine cycle power output. They can be classified into two main categories: water evaporation systems and heat transfer systems. In water evaporation systems, a certain amount of demineralized water is sprayed in to the inlet air stream which evaporates thus decreasing the air temperature. These include evaporative cooling, inlet fogging/air washing, and over-spray systems. According to Ehyaei *et al.* [11], the minimum achievable temperature with these systems, is limited to the ambient wet bulb temperature. In heat transfer systems, the coolant and the air stream do not come into contact; the inlet air cooling involves the use of mechanical chillers, absorption chillers or cold thermal storage systems. Lower air temperatures and therefore larger power outputs can be attained by the heat transfer systems based on refrigeration systems [12].

Barigozzi *et al* [13] conducted techno-economic analysis of gas turbine inlet air cooling of combined cycle power plants operating in three different climatic conditions. The system is based on cold water thermal storage charged by mechanical chillers. Their results show that the best techno-economic performance of the inlet air cooling application is obtained from sites with high ambient temperatures and low relative humidity characterized by high net present values and low pay back time on investment, while wet climates required larger cold storage thus increasing the investment costs. Relative humidity is shown to have a strong influence on the sizing of the cold storage tank.

Najjar and Abubaker [14] performed a thermo-economic analysis of a new form of gas turbine inlet air cooling system, called the indirect evaporative cooling system (IECS). This system is a combination of an air humidifier with a vapor compression mechanical chiller or absorption chiller for cooling part of the total air. Their results show that with combined IECS and mechanical chiller, the power output and thermal efficiency of the gas turbine plant increased by 4% and 2%, respectively in hot and humid weather, while with combined IECS and absorption chiller, the power output and thermal efficiency of the gas turbine plant increased by 11.9% and 9.8%, respectively in hot and humid weather. The thermo economic evaluation show that although the capital cost for the combined IECS and absorption chiller system is the highest, it has the lowest recovery period of 1 year, while the recovery period for the combined IECS and mechanical chiller is 8 years.

Cooling the turbine inlet air can increase the power output substantially. This is because the specific volume of cooled air is smaller, giving the turbine a higher mass flow rate and resulting in increased turbine power output and cycle efficiency [10]. A review by Al-ibrahim and Varnham [6] shows that there are three main inlet air cooling methods: evaporative cooling using evaporative media or water spraying to the inlet air (fogging); cooling by the use of thermal energy storage, chilled water storage or ice harvesting; and cooling the inlet air by the use of refrigeration plant (vapor compression or absorption refrigeration). These techniques have been studied extensively, and are being applied to gas turbine plants around the world.

Dawoud et al. [12] compared these technologies with respect to their effectiveness in power boosting of small-size gas-turbine power plants used in two locations at Marmul and Fahud in Oman. Their findings show that compressor inlet air cooling by fogging generated 11.4% more electric power in comparison to evaporative cooling in both locations. The aqua-lithium bromide absorption cooling produced 40% and 55% more electric power than cooling by fogging at Fahud and Marmul, respectively.

Alhazmy and Najjar [15] compared the use of two different types of air coolers, namely, water spraying system and cooling coil, to improve the performance of gas turbine power plants. Their results show that the water spray (evaporative) coolers operate efficiently in hot and dry climatic conditions, while the cooler coils (typical refrigeration systems) are better suited for use in humid climates. According to Boonnasa et al. [16] the addition of absorption chiller to a CCPP for compressor inlet air cooling could increase the power output of a gas turbine (GT) by about 10.6% and the combined cycle power plant by around 6.24% annually. The result of their economic analysis showed that the payback period will be about 3.81 years, internal rate of return 40%, and net present value 19.44 MUS$. Mohapatra [17] compared the impacts of integrating vapor compression and vapor absorption cooling system to a combined cycle plant for inlet air cooling. Their study show that the vapor compression inlet air cooling improves the CCPP specific power output by 9.02% compared to 6.09% obtained with the vapor absorption cooling. However, to operate the vapor compression system, power is extracted from the gas turbine output.

Due to the increasing focus on water conservation and the environmental effects of both once- through and evaporative cooling, the use of air cooled condensers for rejecting heat in combined cycle power plant is increasing [18]. In combined

cycle power plants (CCPP) with air cooled condensers, heat is rejected directly or indirectly to the ambient air during the condensation process. A drawback of the air cooled condensers is that their performance can decline as ambient temperatures increase and result in decrease in the steam turbine power output. Increased ambient temperature reduces the heat transfer (heat rejection) rate during steam condensation leading to rise in turbine back pressure. As the turbine back pressure increases, the output of the steam turbine decreases [19]. Since air cooled condensers operate with the ambient dry bulb temperature as the theoretical minimum attainable temperature, their efficiency can drop by about 10% when ambient temperatures rise [20, 21].

Chuang and Sue [4] presented the results of a field performance test conducted on an active CCPP with air-cooled condenser operating in Taiwan. The results show that the CCPP can produce more power output when operating at a lower ambient temperature (or lower condenser pressure) and for each 1°C drop in ambient temperature, the power output of the CCPP increased by 0.6% and efficiency improved by 0.1%.

Some approaches have been used or proposed to maintain air cooled condenser performance under higher ambient temperatures. The first approach (the most popular) is to increase the turbine exhaust pressure whereby the condensing temperature is increased. This results in a reduction in net power output of the steam turbine. The second approach is to increase the air flow through the air cooled condenser during the hot period. This approach entails additional energy consumption and over sizing of the fans. The third approach that has been proposed is to cool the air cooled condenser intake air by spraying water. This system requires makeup water and hence, no longer qualifies as a “true” dry cooled system. Incomplete evaporation of water droplets may increase the risk of corrosion, scaling, and environmental discharge violations [20, 21].

In the fourth approach, as proposed by Gadhamshetty and others [20] and Nirmalakhandan and others [21], a sensible heat, low temperature thermal energy storage (TES) system is used to pre-cool the ambient air supply to the air compressor (AC) and the air cooled condenser. The TES system is maintained at the specified temperature by a LiBr-H_2O absorption refrigeration system (ARS) driven by waste heat from the stack gases of the CCPP. A major concern with the TES is the large volume of the storage tank, which is a function of plant capacity as well as the design inlet air temperature to the air cooled condenser. However, both research based their studies on energy analysis of combined cycle plants operating in the arid regions and not in the hot and humid regions

In wet cooling systems, the effectiveness of the evaporative cooling process, is influenced by the relative humidity of the ambient air at the specific location, the higher the relative humidity, the lower the rate of cooling by evaporation [22]. Thus, in hot and humid regions such as Southern Nigeria, latitude 4°45′N and longitude 7°00′E, where the annual average relative humidity is about 80% [23], power plants with air cooled condensers are increasing in number.

Singh [9] performed exergy and energy analysis of an active combined cycle power plant using exhaust heat operated ammonia-water absorption refrigeration system for inlet air cooling. Based on the Indian climatic conditions, the results show that the power output, energy and exergy efficiencies of the plant increased by 9440kW, 1.193% and 1.133% respectively, during the summer season, while the power output increased by 400kW during the winter season. However, this study did not consider the effect of cooling the steam condenser.

Environmental concerns such as air pollution and global warming have amplified the need for environmental impact assessment of thermal power plants. Oyedepo et al.[24] conducted thermo-economic and environmental analysis of 11 gas turbine power plants (GT) in Nigeria. The environmental analysis show that the rate of CO_2 emissions for the GT power plants, varied between 100.18 and 408.78 kgCO_2/MWh, while the cost rate of environmental impact varied from 40.18$/h to 276.97$/h. Parametric analysis show that CO_2 emissions and cost of environmental impact decrease with increasing gas turbine inlet temperature. Memon et al. [25] carried out similar study on simple and regenerative gas turbine power plants. Their results show that the rate of CO_2 emission decrease as the compressor inlet air temperature decreased and the gas turbine inlet temperature increase. A related study by Ahmadi et al. [26] shows that rate of CO_2 emission in a combined cycle power plant can be reduced by using a low fuel injection rate into the combustion chamber.

Therefore, the main aim of this paper is to present thermodynamic, economic and environmental performance assessment of an existing combined cycle power plant (CCPP) retrofitted with a waste heat driven aqua lithium bromide absorption refrigerator for cooling inlet air streams to the compressor and air-cooled steam condenser. The active CCPP operates in the tropical rain forest region of Southern Nigeria at latitude 4°45′N and longitude 7°00′E. The assessment is based on thermodynamic, environmental and economic indications such as the power output, specific fuel consumption, compressor inlet air temperature, flue gas stack exit temperature, thermal efficiency, carbon monoxide (CO), oxide of nitrogen (NOx) and carbon dioxide (CO_2) emissions, annual revenue, net present value, break-even point, and levelized cost of energy, among others

Parametric variations were considered to determine the impact of ambient conditions on the performance of the combined cycle power plant. A chilled water circulation arrangement to reduce the volume requirement of the chilled water is considered. It is expected that the results of this study will encourage owners of combined cycle power plants in hot and humid regions such as Nigeria, to make appropriate modifications to their plants for improved performance, economic and environmental benefits. The results and simulations were generated using the MATLAB and Engineering Equation (EES) software.

2. Problem Formulation and Solution Methods

The system diagrams, principles of operation and the thermodynamic modeling of the existing power plant and absorption refrigeration system are presented in this section.

2.1. System Description

The proposed system is made up of the gas-turbine cycle unit (GTC), the steam-turbine cycle unit (STC), and the absorption refrigeration cycle unit (ARC). The first two units are the existing combined (gas- and steam-) cycle thermal power plant (CCPP), which is to be retrofitted to include a waste-heat-driven H_2O-LiBr absorption refrigerator to provide all the cooling load required by the power plant, Figure 1.

The CCPP consists of: three natural gas fired gas turbine (GT) units; three dual pressure, forced circulation heat recovery steam generators (HRSG); a dual pressure steam turbine (ST) unit with one high pressure and two low pressure double and phase diagrams of the CCPP are shown in Figures 1 and 2. In the combined cycle power plant, inlet air at the ambient temperature (state 1) is compressed by the air compressor (AC) to state 2 before entering the combustion chamber (CC) where it mixes and reacts with the natural gas from the fuel supply system to produce hot flue gases, which exit the CC and enter the gas turbine (GT). The flue gases expand in the GT from state 3 to state 4, producing power for driving the air compressor (AC) and for conversion into electricity in the electric generator (el.Gen1).

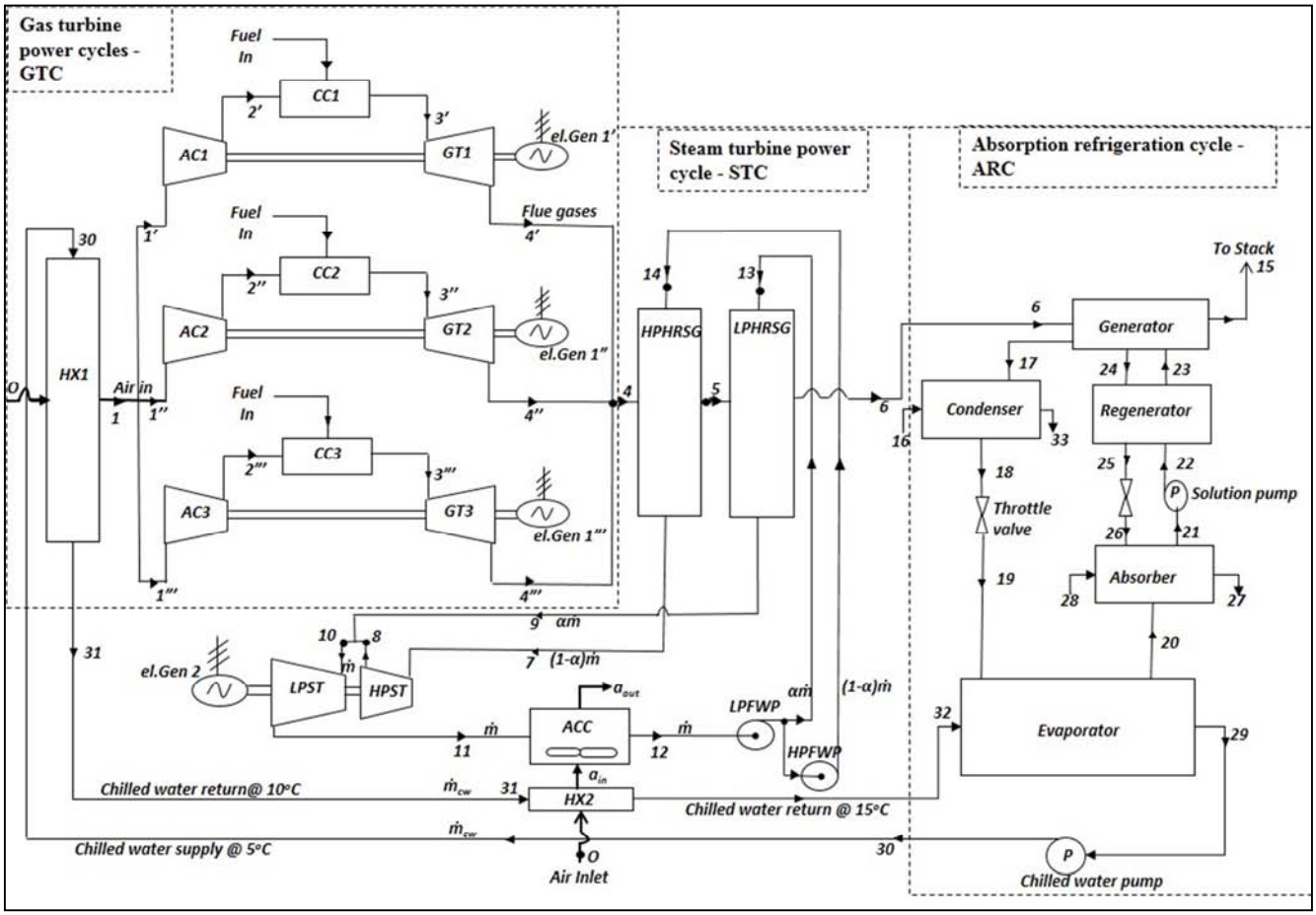

Figure 1. Plant diagram of the proposed combined cycle power and refrigeration plant.

The exhaust flue gases at state 4 pass through the heat recovery steam generator (HRSG) where high- and low-pressure (HP and LP) feed water streams are heated to states

7 and 9, respectively, as the flue gases exit the HPHRSG and LPHRSG at states 5 and 6, respectively. The superheated steam from the HPHRSG at state 7 expands in the high pressure turbine (HPST) to state 8, and mixes with the superheated steam from the LPHRSG at state 9 to form a homogenous steam mixture at state 10 before expanding in the low pressure steam turbine (LPST) to state 11. The mechanical power from the steam turbines is converted into electrical power in the electrical generator 2 (el. Gen 2). The exit wet steam is condensed in the air cooled steam condenser (SC) to saturated liquid water at state 12 before being pumped by the low pressure feed water pump (LPFWP) to state 13. One part of this low pressure feed water ($\alpha\dot{m}$) is fed into the LPHRSG, while the remaining part ($(1-\alpha)\dot{m}$) is pumped by the high pressure water pump (HPFWP) to state 14 and fed into the HPRSG for the dual-pressure steam turbine cyclic process to continue repeating.

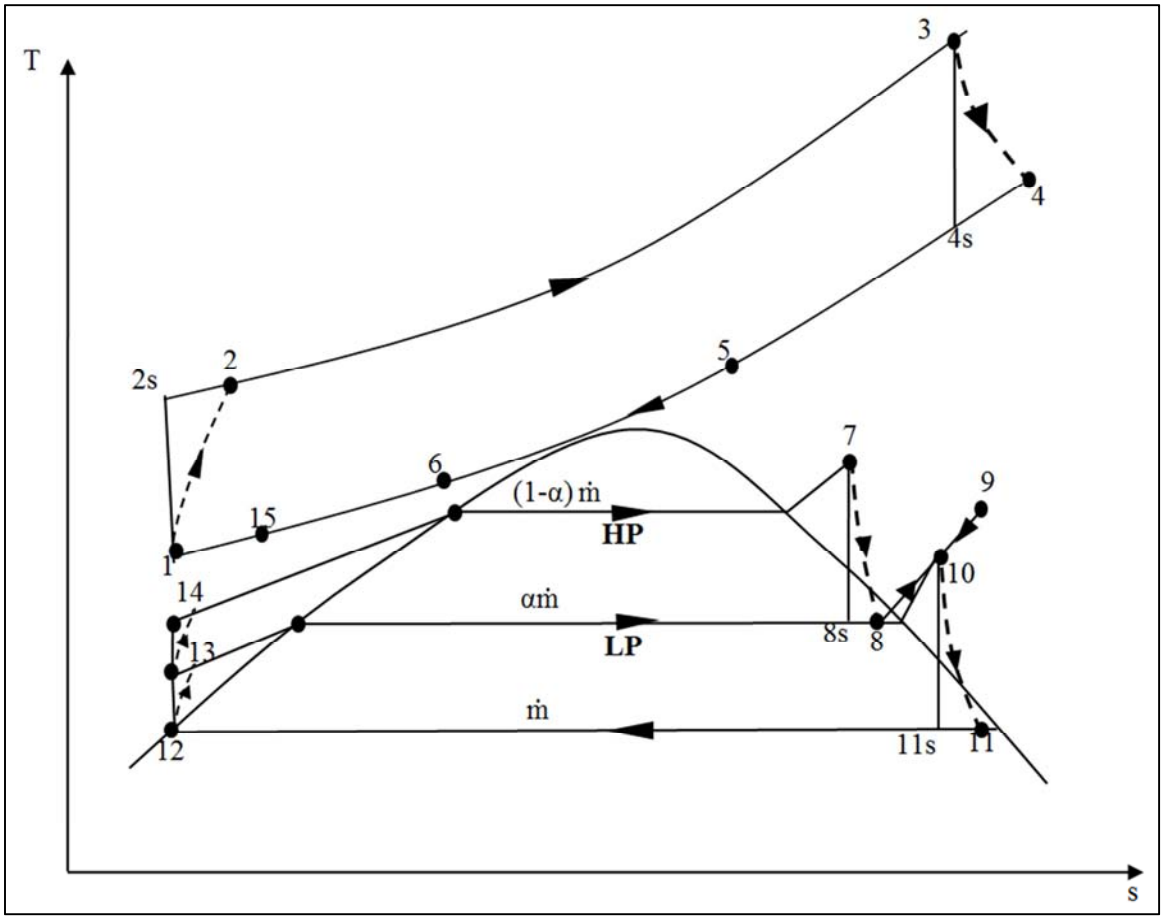

Figure 2. T-s diagram of the combined power cycle showing the relevant thermodynamic processes in the gas- and steam-turbine cycles.

At state 6, the exhaust flue gases exiting the HRSG units are used to power the LiBr-H_2O absorption refrigeration unit (ARC) and then discharged at state 15 into the atmosphere. The ARC consists of a generator, regenerator, absorber, condenser, evaporator, solution feed pump and two expansion valves. Dilute LiBr-H_2O solution in the absorber is pumped from state 21 through the regenerator to the generator at 23. In the refrigerant generator, the diluted solution is heated directly by the exhaust gases. A large portion of water in the LiBr-H_2O solution is evaporated. The generated pure water vapor enters the refrigerant condenser, while the concentrated LiBr–H_2O solution at state 24 returns to the absorber through the regenerator (state 25) and throttle valve (state 26). The evaporated refrigerant (water) vapor at state 17 is condensed as it passes through the condenser to state 18, throttled to low pressure and temperature to state 19, before entering the evaporator, where it is evaporated by the heat from the circulating water from the air cooling coils to state 20. The saturated refrigerant vapor from the evaporator at state 20 enters the absorber, where it is absorbed by the concentrated solution from the generator at state 26. The resulting diluted solution at state 20 is pumped to the generator through the regenerator to complete the absorption refrigeration cycle.

Chilled water pump circulates chilled water at 5°C from the evaporator (state 29) through an air cooler / heat exchanger (HX1) to cool the inlet air (state 1) to the air compressors (AC). During this heat exchange process the temperature of chilled water increases to 10°C. The same volume of chilled

water (now at 10°C) flows from state 31 through another air cooler (HX2) to cool the inlet air (a_{in}) to the air cooled steam condenser (ACC); gaining more heat to reach 15°C. Finally the chilled water returns to the evaporator where it is cooled to 5°C by the ARC and the cycle continues repeating.

As the inlet air stream is cooled from the given ambient conditions at the plant location, the air temperature drops while the relative humidity gradually rises, as shown Figure 3.

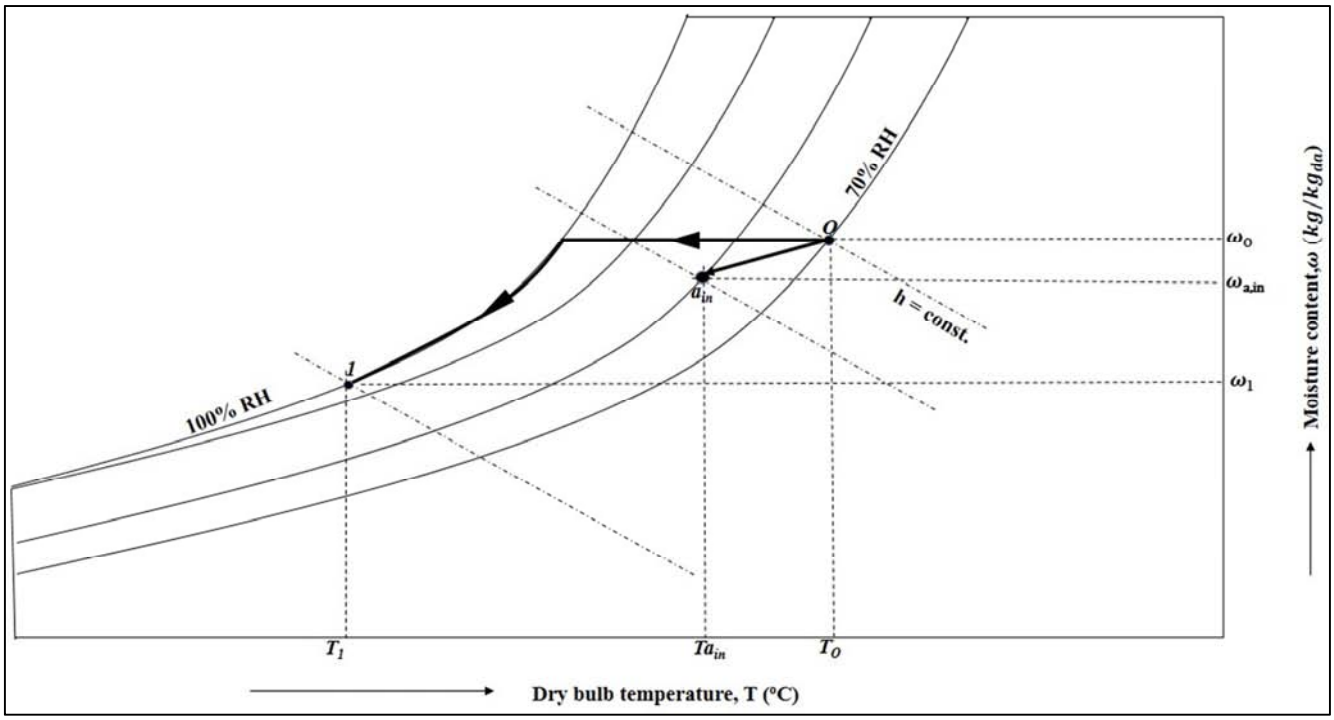

Figure 3. Psychrometric chart of the compressor and steam condenser inlet air cooling processes.

2.2. Thermodynamic Analysis of the Combined Cycle Power Plant

The thermodynamic assessment of the active combined cycle power plant is here conducted with actual operating data. The major units of the combined cycle power plant undergo different thermodynamic processes as represented on the T – s diagram shown in Figure 2. The assumptions made doing the analysis includes:

a. Mass and energy flow through the plant is in steady state.

b. Changes in kinetic and potential forms of energy are negligibly small.

c. All gases (air and flue gases) behave like ideal gases.

d. Heat losses and mechanical losses were neglected.

e. Air and water enter the system at ambient temperature and pressure

f. The thermodynamic equations are derived for the major thermodynamic devices by treating them as control volumes

g. The mass flow rates and thermodynamic characteristics of the three gas turbine units are identical, so that only one is analyzed and the extensive outputs are multiplied by a factor of 3.

2.2.1. The Gas Turbine (Brayton) Cycle

The conventional gas turbine plant runs on the Brayton cycle where both the compression and expansion processes take place in rotating machinery. Using Figure 2, the thermodynamic models for the major units are derived as follows [7], [15], [27]–[32]

(i) Air Compressor

The power required to drive the compressor is given as

$$\dot{W}_{i,AC} = \dot{m}_2(h_2 - h_1) = \dot{m}_a c_{pa}(T_2 - T_1) \quad (1)$$

where $\dot{m}_a$ (kg/s) is the mass flow rate of the air through the compressor; $\dot{W}_{i,AC}$ (kW) is the ideal compression power; c_{pa}(kJ/kg.K) is the isobaric specific heat capacity of the air; h_1, h_2 (kJ/kg) are the specific enthalpies at entry and exit of the compressor, respectively; T_1, T_2 (K) are the temperatures of air at entry and exit of compressor, respectively.

The actual compressor power is given as

$$\dot{W}_{a,AC} = \frac{\dot{W}_{i,AC}}{\eta_{s,AC}} \quad (2)$$

where the isentropic efficiency of the compressor, $\eta_{s,AC}$ $(-)$is

given as

$$\eta_{s,AC} = 1 - \left(0.04 + \frac{(P_2/P_1)-1}{150}\right) \quad (3)$$

where P_1, P_2 (kPa) are the compressor inlet and exit air pressures, respectively.

The specific heat capacity of the air is given as [1]

$$c_{pa} = 1.0189134 * 10^3 - 1.3783636*10^{-1}\, T + 1.9843397*10^{-4}\, T^2 + 4.2399242*10^{-7}\, T^3 - 3.7632*10^{-10}\, T^4 \quad (4)$$

(ii) Combustion Chamber

The rate of heat addition in the combustion chamber is given as [7]

$$\dot{Q}_{cc} = \dot{m}_f[\eta_{cc}\, LHV + SH_f] = \dot{m}_f\,[\eta_{cc}\, LHV + c_{pf}\,(T_f - T_i)] \quad (5)$$

where $\dot{m}_f$ (kg/s) is the fuel mass flow rate; η_{cc} $(-)$ is the combustion efficiency and accounts for the incomplete combustion and heat losses in the combustion chamber; LHV (kJ/kg) is the lower heating value of the fuel gas at the initial temperature; SH_f (kJ/kg) is the increase in sensible enthalpy of the fuel gas due to preheating before entry to combustion chamber; T_i (K) is the fuel gas initial temperature before preheating; T_f(K) is the temperature of gas after preheating /entry to combustion chamber and c_{pf} (kJ/kg. K) is the specific heat capacity of the fuel (natural gas):

$$c_{pf} = \sum_{i=1}^{n} \mathrm{y_i}\, c_{pfi} \,/\, M_i \quad (6)$$

where $\mathrm{y_i}$, M_i(kg/ kmol. K) and c_{pfi} (kJ/ kmol. K) are the mass fraction, the molar mass and the isobaric specific heat capacity of the i[th] gas component, respectively.

This can be determined from the natural gas composition analysis as follows:

$$c_{pfi} = \mathrm{a} + \mathrm{b}\, T_{a,v} + \mathrm{c}\, T_{a,v}^{\ 2} + \mathrm{d}\, T_{a,v}^{\ 3} \quad (7)$$

where a, b, c, d are coefficients which can be obtained from standard tables given in [33].

$T_{a,v} = \frac{T_f + T_i}{2}$ (K) is the average temperature of the natural gas

The specific heat capacity of the flue gases, c_{pg} $(\frac{kJ}{kg}.K)$ is given as

$$c_{pg} = 0.991615 + 6.99703 \times 10^{-5} T + 2.7129 \times 10^{-7}\, T^2 - 1.22442 \times 10^{-10}\, T^3 \quad (8)$$

(iii) The Gas Turbine

The ideal and actual turbine powers are given respectively, as

$$\dot{W}_{s,GT} = \dot{m}_g(h_3 - h_4) = \dot{m}_g c_{pg}(T_3 - T_4) \quad (9)$$

and

$$\dot{W}_{a,GT} = \dot{W}_{s,GT}\, \eta_{s,GT} \quad (10)$$

The turbine isentropic efficiency, $\eta_{s,GT}$ (-) is given as [15]

$$\eta_{s,GT} = 1 - \left(0.03 + \frac{(P_2/P_1)-1}{180}\right) \quad (11)$$

T_4, T_3 are turbine inlet and exit flue gas temperatures respectively.

The rate of heat transfer associated with the turbine exit flue gas is given as

$$\dot{Q}_{GT,exit} = \dot{m}_g c_{pg}(T_4 - T_1) = (1 - \eta_{I,GTC})\dot{Q}_{cc} \quad (12)$$

The integral characteristics of the gas turbine power plant

The gas turbine net power output, $\dot{W}_{net,GTC,}$ and cycle thermal efficiency ($\eta_{I,GT}$) are respectively, given as

$$\dot{W}_{net,GTC} = \dot{W}_{a,GT} - \dot{W}_{a,AC} \quad (13)$$

and

$$\eta_{I,GTC} = \frac{\dot{W}_{net,GTC,}}{\dot{Q}_{cc}} \quad (14)$$

Specific fuel consumption,

$$SFC_{gt} = \frac{3600\, \dot{m}_f}{\dot{W}_{net,GTC}}\ (\mathrm{kg/\ kWh}) \quad (15)$$

2.2.2. The Steam Turbine (Rankine Cycle) Power Plant

The steam turbine power plant operates on the Rankine cycle. The major thermodynamic devices of the steam turbine plant are, the HRSGs, the steam turbine, the condenser and the feed water pumps. Following Figure 2, thermodynamic models for the major devices are given as follows:

(i). Heat Recovery Steam Generators (HRSGs)

The dual pressure steam cycle has high and low pressure HRSGs (HPHRSG and LPHRSG), the individual and total heat transfer rates are given respectively as

$$\dot{Q}_{HPHRSG} = (1 - \alpha)\dot{m}(h_7 - h_{14}) = \dot{m}_g c_{pg}(T_4 - T_5) \quad (16)$$

$$\dot{Q}_{LPHRSG} = \alpha\dot{m}(h_9 - h_{13}) = \dot{m}_g c_{pg}(T_5 - T_6) \quad (17)$$

and

$$\dot{Q}_{HRSG} = \dot{Q}_{HPHRSG} + \dot{Q}_{LPHRSG} = \dot{m}_g c_{pg}(T_4 - T_6) = \dot{m}[(1-\alpha)(h_7 - h_{14}) + \alpha(h_9 - h_{13})] \quad (18)$$

where $\dot{Q}_{HRSG}$ (kW) is the heat transfer rate in the HRSG from the gas turbine exit flue gases to the feed water streams; $\dot{Q}_{HPHRSG}(kW)$ is the heat transfer rate in the HPHRSG; $\dot{m}_{HP} = (1-\alpha)\dot{m}$ is the mass flow rate of high pressure feed water flowing through the HPHRSG; $\dot{Q}_{LPHRSG}$ is the heat transfer rate in the LPHRSG, $\dot{m}_{LP} = \alpha\dot{m}$ is the mass flow rate of water flowing through the LPHRSG; α (-) is the mass fraction of steam circulating in the low pressure circuit.

$$\alpha = \frac{\dot{m}_{LP}}{\dot{m}} = \frac{\dot{m}_{LP}}{\dot{m}_{LP} + \dot{m}_{HP}} \quad (19)$$

(ii). Steam Turbine

The total power output from the low and high pressure steam turbines is given by:

$$\dot{W}_{st} = \eta_{s,ST}[(1-\alpha)\dot{m}(h_7 - h_8) + \dot{m}\,(h_{10} - h_{11})] \quad (20)$$

where $\eta_{s,ST}(-)$ is the steam turbine isentropic efficiency.

(iii). Air Cooled Condenser

Following the work of Donovan and Grimes [34] the air cooled condenser analysis is performed. The analysis is based upon the assumption that only isothermal heat rejection occurs during condensation, the amount of heat rejected to condense steam to liquid water is totally absorbed by the cooling air, with sensible heat rejection (sub cooling) neglected. The energy balance across the ACC:

$$\dot{Q}_{Cond} = \dot{m}(h_{11} - h_{12}) = \dot{m}_{acc}\, c_{pa}\,(T_{a,out} - T_{a,in}) \quad (21)$$

$\dot{m}_{acc}$, c_{pa}, $T_{a,in}$, $T_{a,out}$ are the mass flow rate of the ambient air inlet to ACC, specific heat of the air, inlet air temperature and the air exit temperature from the ACC respectively. The air exit temperature can be determined as

$$T_{a,out} = \frac{\dot{m}(h_{11} - h_{12}) + \dot{m}_{acc}\, c_{pa}\, T_{a,in}}{\dot{m}_{acc}\, c_{pa}} \quad (22)$$

The effectiveness of a cross-flow air-cooled heat exchanger is defined by;

$$\mathcal{E} = \frac{T_{a,out} - T_{a,in}}{T_{11} - T_{a,in}} \quad (23)$$

$T_{11}\,(K)$ is the steam temperature at the condensing pressure (turbine back pressure)

$$T_{11} = \frac{T_{a,out} - T_{a,in}}{\mathcal{E}} + T_{a,in} \quad (24)$$

The quality of the turbine exhaust steam in to the condenser is given as

$$X = \frac{h_{11} - h_{12}}{h_{11g} - h_{12}} \quad (25)$$

h_{11g} (kJ/kg) is the specific enthalpy of saturated vapor at the condensing pressure

(iv). Feed Water Pumps

The power consumption of the high and low feed water pumps is given as:

$$\dot{W}_{FWP} = \frac{\dot{m}\,[(h_{13} - h_{12}) + (1-\alpha)\,(h_{14} - h_{13})]}{\eta_{s,FWP}} \approx \frac{\dot{m}\, v_{12}[(P_{13} - P_{12} + (1-\alpha)(P_{14} - P_{13})]}{\eta_{s,FWP}} \quad (26)$$

where $\eta_{s,FWP}\,(-)$ is the high and low feed water pump isentropic efficiency.

(v). The Integral Characteristics of the Steam Turbine Power Plant

The net power output of the dual pressure steam turbine cycle, $\dot{W}_{net,STC}\,(kW)$ becomes

$$\dot{W}_{net,STC} = \dot{W}_{net,ST} - \dot{W}_{FWP} \quad (27)$$

The thermal efficiency of the steam turbine cycle is given as:

$$\eta_{I,STC} = \frac{\dot{W}_{net,STC,}}{\dot{Q}_{HRSG}} \quad (28)$$

2.2.3. Thermodynamic Modeling of the LiBr – H_2O Absorption Refrigeration Cycle

Following the works of Dincer et al [35], Dincer and Ratlamwala [36], Popli et al. [37], Touaibi et al. [38], Kaushik and Arora [39] and Muhsin and Kaynakli [40], the ARC is analyzed based on Figures 1 and 2 as presented below. The following assumptions were made in conducting the energy analysis of the LiBr – H_2O absorption refrigeration cycle:

a. Mass and energy flow through the system is in steady state.

b. Solution leaving the absorber and the generator are assumed to be saturated and in equilibrium conditions at their operating temperatures and concentrations.

c. The refrigerant states leaving the condenser and evaporator are also assumed to be saturated

(i). Refrigerant Generator

Energy balance across the generator is given as

$$\dot{Q}_{gen} = \dot{m}_{rf}h_{17} + \dot{m}_{ws}h_{24} - \dot{m}_{ss}h_{23} = k\dot{m}_g c_{pg}(T_6 - T_{15}) \quad (29)$$

where k is the number of turbines in the gas turbine power unit, in this case,$k = 3$;$\dot{m}_{rf}$,$\dot{m}_{ws}$, $\dot{m}_{ss}$ and $\dot{m}_g$(kg/s) are the mass flow rates of the refrigerant (water vapor evaporated in the generator), weak solution, strong solution, and flue gases, respectively.

(ii) Refrigerant Condenser

The rate of heat rejected in the condenser where saturated water vapor (refrigerant) from the generator is cooled to saturated liquid at the generator pressure is given as:

$$\dot{Q}_{cond} = \dot{m}_{rf}\,(h_{17} - h_{18}) \quad (30)$$

(iii) Throttle Valves

The pressure of liquid refrigerant at generator pressure is reduced isenthalpically to the evaporator pressure, $h_{18} = h_{19}$ and $h_{25} = h_{26}$;

(iv) Refrigerant Evaporator

The liquid refrigerant at low pressure is evaporated by the circulating chilled water used for inlet air cooling in the air cooling coil (ACC), and becomes saturated vapor. The refrigeration (or cooling) load, $\dot{Q}_{CL}$ (kW), is given as

$$\dot{Q}_{Evap} = \dot{m}_{rf}(h_{20} - h_{19}) = \dot{Q}_{CL} \quad (31)$$

(v) Refrigerant Absorber

In the absorber, the weak solution from the generator which has been throttled to the absorber pressure readily absorbs the saturated refrigerant vapor from the evaporator to become a strong solution. This exothermic process releases some heat, which is removed by the cooling fluid flowing through the absorber. The rate of heat rejection from the absorber is given as

$$\dot{Q}_{abs} = (\dot{m}_{rf}h_{20} + \dot{m}_{ws}h_{26}) - (\dot{m}_{ss}h_{21}) = \dot{m}_{abs}(h_{27} - h_{28}) \quad (32)$$

where $\dot{m}_{abs}$ (kg/s) is the mass flow rate of the cooling fluid in the absorber.

(vi) Solution Pump

The pump transfers the strong LiBr-H_20 solution from the absorber to the generator, and its power consumption, which is usually negligibly small, is given as

$$\dot{W}_{sp} = \dot{m}_{ss}(h_{22} - h_{21}) \quad (33)$$

(vii) Regenerator

The regenerator heats the strong solution from the absorber on its way to the generator and cools the weak solution returning from the generator to the absorber. The regenerator heat and exergy destruction rates are, respectively

$$\dot{Q}_{reg} = \dot{m}_{ws}(h_{24} - h_{25}) = \dot{m}_{ss}(h_{23} - h_{22}) \quad (34)$$

(viii) Coefficient of Performance of the Absorption Refrigeration Cycle

$$COP = \frac{\dot{Q}_{Evap}}{\dot{Q}_{gen} + \dot{W}_{sp}} \quad (35)$$

2.3. Inlet air Cooling Load Analysis

The total cooling load comprises of the heat removed to reduce the ambient air temperature from its initial ambient condition to the desired cooled state, i.e. the sensible heat of air and the heat required to condense the moisture contained in the air (the latent heat). Thus, the total inlet air cooling load or the refrigerating capacity, $\dot{Q}_{CL}$ (kW), is the summation of both the sensible ($\dot{Q}_s$) and the latent ($\dot{Q}_L$) cooling loads:

$$\dot{Q}_{CL} = \dot{Q}_s + \dot{Q}_L = \dot{Q}_{Evap} \quad (36)$$

The sensible cooling load can be determined as [12]

$$\dot{Q}_s = \frac{\dot{V}_a}{v_a} c_{pa}(T_0 - T_1) \quad (37)$$

$\dot{V}_a$(m^3/s) is volume flow rate of air based on actual data acquired from the plant; T_0(K) is the dry bulb temperature of the ambient air; and T_1 (K) is the cooled air temperature at state 1; v_a(m^3/kg) is the specific volume of the humid air per kilogram of dry air.

The specific volume of humid air per kilogram of dry air may be given as [12]

$$v_a = (0.287 + \omega_O\ 0.462)\frac{T}{P_{atm}} \quad (38)$$

where T (K) is the dry bulb temperature; P_{atm} (kPa) is the atmospheric pressure; $\omega_O(kg_{wv}/kg_{da})$ is the specific humidity of the air which is given by [33] [41]

$$\omega_O = \frac{0.622\ RH_O}{(P_{atm} - RH_O)} P_{wv} \quad (39)$$

where P_{wv} (kPa) is the saturation water vapor pressure at the given dry bulb temperature, T; $RH_O(-)$ is the relative humidity of the air.

The latent cooling load, $\dot{Q}_L$ (kW), is given as

$$\dot{Q}_L = \frac{\dot{V}_a}{v_a}\left[\omega_O\left(c_{pv}T_O + h_{fg}\right) - \omega_1\,(c_{pv}T_1 + h_{fg}) - (\omega_O - \omega_1)\,c_{pw}T_1\right] \quad (40)$$

where c_{pv} (kJ/kg. K) is the isobaric specific heat capacity of water vapor in the humid air; h_{fg} (kJ/kg) is the air latent heat of evaporation of water at 0°C; ω_1(kg/kg. da) is the specific humidity of the air at the desired compressor inlet temperature; and c_{pw}(kJ/kg. K) is the isobaric specific heat

capacity of liquid water.

The mass flow rate of chilled water circulating from the evaporator through the air coolers, $\dot{m}_{cw}$ (kg/s), is given as

$$\dot{m}_{cw} = \frac{\dot{Q}_{CL}}{C_{pw}\,(T_{32} - T_{29})} \quad (41)$$

where T_{29} is the chilled water supply temperature and T_{32} is the water return temperature.

The pump power required for chilled water circulation ($\dot{W}_{cwr}$) is given as:

$$\dot{W}_{cwr} = \frac{\dot{m}_{cwr}\,\Delta P}{\rho} \quad (42)$$

ρ (kg/m^3) is the density of water and ΔP (kPa) is the pressure loss to be overcome by the pump.

2.4. Overall Performance Characteristics of the CCPP with and without inlet air cooling to Compressor and Condenser

The overall combined cycle power output and thermal efficiency are given respectively as:

$$\dot{W}_{CCPP_k} = \dot{W}_{net,GTC} + \dot{W}_{net,STC} - \dot{W}_{cwr} \quad (43)$$

$$\eta_{I,CCPP} = \frac{\dot{W}_{CCPP}}{\dot{Q}_{cc}} \quad (44)$$

2.5. Economic Modelling

The equations for conducting the economic performance assessment of the combined cycle power plant configurations, with and without inlet air cooling are presented in this section. The capital cost of each plant configuration is estimated by summing up the capital cost of each major component.

The capital cost of combined power plant, C_k ($US\$$), is determined from

$$C_k = \sum_j C_j\, W_j \quad (45)$$

where C_j () is the unit cost per output of the plant component; W_j () is the net output or rated capacity of the plant component such as gross power output, ton refrigeration, thermal load or mass flow rate; j is the plant component such as CCPP, ARC, HX1, HX2 and chilled water pump; k is the particular plant configuration, with or without inlet air cooling.

The annual operating and maintenance cost, OM_k ($US\$/yr$), is given as

$$OM_k = \left[\sum_j \left(FOM_j + VOM_j\right) W_j + C_{fuel}\right] Ops \quad (46)$$

where FOM_j and VOM_j are the fixed and variable operating and maintenance cost rates per output of the j^{th} component of the plant, respectively;C_{fuel} is the hourly cost rate of fuel and Ops is the total hours of operation per year

The annual revenue from a plant, R_k ($US\$/yr$), is given as [42]

$$R_k = (C_{el}\dot{W}_{net,k})Ops \quad (47)$$

where C_{el} is the unit price per kWh (electricity tariff) of electricity (\$/kWh);$\dot{W}_{net,k}$ is the net total power output of the k^{th} plant (kW).

The life cycle cost of the thermal plant configuration, LCC_k ($US\$$), is given as [43]

$$LCC_k = C_k + \left[OM_k \times \frac{(1+I_r)^N - 1}{I_r\,(1+I_r)^N}\right] \quad (48)$$

where N is economic life of the plant (Years)

The annualized life cycle cost, $ALCC_k$ (\$/yr.), is as [44]

$$ALCC_k = LCC_k \times \left[\frac{1}{\frac{(1+I_r)^N - 1}{I_r\,(1+I_r)^N}}\right] \quad (49)$$

The levelized cost of energy production of each plant, $LCOE_k$ (\$/kWh), is given as [43], [45]

$$LCOE_k = \frac{ALCC_k}{\dot{W}_{net,k} \times Ops} \quad (50)$$

The break-even point of each plant configuration, BEP_k (yr), is given as [44]

$$BEP_k = \frac{LCC_k}{R_k} \quad (51)$$

The net present value of each plant configuration, NPV_k ($US\$$), is given as [43], [46]

$$NPV_k = -C_k + \left[(R_k - OM_k) \times \frac{(1+I_r)^N - 1}{I_r\,(1+I_r)^N}\right] \quad (52)$$

2.6. Environmental Modelling

In order to properly assess the environmental impact of thermal power plants, the emissions of CO, CO_2 and NO_x are considered. The amount of CO and NO_x produced in the combustion chamber due to the combustion reaction depends on various combustion characteristics including the adiabatic flame temperature. Following the works of Rizk and Mongia [47], Lazzaretto and Toffolo [48], Ahmadi and Dincer [49], Ehyaei and others [50] and Ganjehkaviri and others [51]; the rates of CO_2, NOx, and CO emitted are determined as now described.

The mass flow rate of CO_2 emission, $\dot{m}_{CO2}(kg_{CO2}/s)$, and specific carbon dioxide emission (CO_2) emitted per MWh of energy output), sCO_2e (kg_{CO2}/MWh), are, respectively, given as

$$\dot{m}_{CO2} = M_{CO2} x_c \left(\frac{\dot{m}_f}{M_f}\right) \quad (53)$$

and

$$sCO_2e = 3600\left(\frac{\dot{m}_{CO2}}{\dot{W}_{net}}\right) \quad (54)$$

where x_c (-) is the mole fraction of carbon in the fuel; $\dot{m}_f$ (kg/s) is the mass flow rate of the fuel; and M_{CO2} = 44.01 and M_f (kg/kmol) are the molar masses of CO_2 and fuel, respectively.

NOx and CO emissions rates, $\dot{m}_{NOx}$ and $\dot{m}_{CO}$ (kg/s), due to combustion reaction are, respectively, given as

$$\dot{m}_{NOx} = \frac{0.15\times10^{16}\,\tau^{0.5} exp^{\left(\frac{-71100}{Tpz}\right)}}{{P_3}^{0.05}\left(\frac{\Delta P_3}{P_3}\right)^{0.5}} \times \frac{\dot{m}_f}{1000}\left[\frac{kg}{s}\right] \quad (55)$$

and

$$\dot{m}_{CO} = \frac{0.179\times10^{6}\, exp^{\left(\frac{7800}{Tpz}\right)}}{{P_3}^{2}\tau\left(\frac{\Delta P_3}{P_3}\right)^{0.5}} \times \frac{\dot{m}_f}{1000}\left[\frac{kg}{s}\right] \quad (56)$$

For the expressions above, τ, is the residence time in the combustion zone (assumed constant and equal to 0.002s) [52]; P_3 (kPa) is the combustion chamber inlet pressure; and $\Delta P_3/P_3$ is the non-dimensional pressure drop in the combustion chamber; $T_{pz}\,(K)$ is the adiabatic flame temperature in the primary zone of the combustion chamber.

The adiabatic flame temperature is given as [53]

$$T_{pz} = A\,\sigma^{\alpha}\exp(\beta(\sigma+\lambda)^2)\pi^x\theta^y\Psi^z \quad (57)$$

where $\pi = P_3/P_{ref}\,(-)$ is a dimensionless pressure; P_{ref} is the environmental reference pressure, P_{ref} =101.325 kPa; $\theta = T_2/T_{ref}\,(-)$; is a dimensionless temperature; T_2 (K) is the combustion inlet temperature; T_{ref} is the environmental reference pressure, T_{ref} =298 K; Ψ is the fuel hydrogen/carbon atom ratio, for methane, Ψ = 4 [48]; $\sigma = \varphi$, for $\varphi \leq 1$ and $\sigma = \varphi - 0.7$ for $\varphi \geq 1$ (φ is the fuel-air equivalence ratio of the combustion process); x, y, z are quadratic functions of σ, given by the following system of simultaneous quadratic equations:

$$x = a_1 + b_1\sigma + c_1\sigma^2 \quad (58)$$

$$y = a_2 + b_2\sigma + c_2\sigma^2 \quad (59)$$

$$z = a_3 + b_3\sigma + c_3\sigma^2 \quad (60)$$

$A, \alpha, \beta, \lambda, a_i, b_i, c_i$ are constants whose values were tabulated and presented in the works of Ahmadi et al. [53] and Ganjehkaviri et al. [52].

3. Results and Discussion

Based on the models presented in section 2, the results obtained and sensitivity testing are presented and discussed in this section.

3.1. Data Used for the Generation of the Results

The operating log data of the active combined cycle power plant (CCPP) and other thermodynamic, economic and environmental specifications used in this study are presented in Table 1.

Table 1. Input data for the analysis of the combined cycle power and refrigeration plant.

Plant unit	Parameter	Symbol	Units	Value
Operating data of the existing CCPP [54]				
Compressor	Inlet temperature	T_O	°C	30
	Relative humidity of air	RH_O	%	70
	Inlet air pressure	P_1	kPa	99
	Volume flow rate of air(x3)	V_1	m^3/s	1287
Combustion chamber	Inlet air pressure	P_2	kPa	1380
	Fuel inlet temperature	T_f	°C	60.2
	Fuel inlet pressure	P_f	kPa	2650
	Fuel mass flow rate(x3)	$\dot{m}_f$	kg/s	25.83
	Fuel lower heating value	LHV	kJ /kg	52580
Gas turbine	Outlet temperature of flue gases	T_4	°C	531
	Net power output(x3)	$\dot{W}_{net,GTC}$	MW	447
	Flue gas mass flow rate(x3)	$\dot{m}_g$	kg/s	1509.3
HRSG	Stack exhaust temperature	T_6	°C	126
Steam turbine	Net power output	$\dot{W}_{net,STC}$	MW	202
	Inlet steam high pressure (HP)	P_7	kPa	10020
	Inlet steam low pressure (LP)	P_{10}	kPa	537
	Mass flow rate of HP steam	$\dot{m}_{SHP}$	kg/s	175.2
	Mass flow rate of LP steam	$\dot{m}_{SLP}$	kg/s	54.7
	Inlet temperature of HP steam	T_7	°C	512

Plant unit	Parameter	Symbol	Units	Value
	Inlet temperature of LP steam	T_{10}	°C	257.2
Air cooled condenser	Inlet wet steam temperature	T_{11}	°C	60.7
	Inlet saturated water pressure	P_{12}	kPa	21
	Air mass flow rate	$\dot{m}_{ca}$	kg/s	160680
Other thermodynamic specifications				
	Combustion efficiency [55]	η_{CC}	–	0.98
	Flue gas constant	R_g	kJ/kg. K	0.285
	Steam turbine isentropic efficiency [28]	$\eta_{s,ST}$	-	0.82
	Feed pump isentropic efficiency	$\eta_{s,FWP}$	-	0.90
	Desired compressor inlet air temp. [16]	T_1	°C	15
	Air relative humidity at cooling coil exit	RH_1	%	100
	Density of chilled water	ρ	kg/m^3	1000
	Pressure loss overcome by chilled water circulation pump	ΔP	kPa	9.8 x 10^5
	Chilled water supply temperature	T_{29}	°C	5
	Chilled water return temperature	T_{32}	°C	15

Economic specifications

Combined cycle power plant -dry cooled (with air cooled condenser) [56], [57]	Capital cost	$/kW	1200
	Fixed O & M cost	$/kW	13.2
	Variable O & M cost	$/MWh	3.6
Absorption Refrigeration system [50] [58]	Capital cost	$/ton	1000
	O & M costs	$/yr.	4% of capital cost
Air cooling coil (heat exchanger, HX) [13]	Capital cost	$/kW	195
	O&M Costs		4% of Capital cost
Water pump [59]	Capital cost	$ / kW	$881W_p^{0.4}$
	Annual hours of operation	hours	8000
	Economic life	years	20
Others [60]–[63]	Interest rate in Nigeria (August, 2016)	%	14
	Electricity tariff in Nigeria (August, 2016)	$/kWh	0.0780
	Cost of natural gas	$/kg	0.096

3.2. Validation of Models for the Existing Combined Cycle Power Plant (CCPP)

Using the fuel heat input rate of 1333MW, key performance characteristics of the existing combined cycle power plant were computed. These computed values were compared with their corresponding measured operating values of the active CCPP, Table 2. The error margins were within the acceptable range for power plant applications.

Table 2. Comparison of measured and computed characteristics of the existing CCPP.

Parameter	Measured data	Computed value	Error (%)
Gas turbine net power output (MW)	447.0	441.3	1.28
Gas turbine exit temperature (°C)	531.3	527.5	0.72
Gas turbine outlet mass flow (kg/s)	1509.3	1476.3	2.19
Steam turbine power output (MW)	202.3	200.2	1.04
HRSG exit flue gases temperature (°C)	126.0	123.9	1.67

3.3. Thermodynamic Characteristics of the Combined Power Plant and Absorption Refrigeration System

The computed key performance parameters of the gas turbine cycles, steam turbine cycle, and the combined power cycle plant, with and without inlet air cooling are tabulated in Table 3. It clearly shows that by cooling the inlet air to the compressors to 15°C, the net power output of the gas turbine cycles increased by 48.3MW, and by cooling the inlet air streams to the air cooled steam condenser to 29°C, the net power output of the steam turbine cycle increased by 1.4MW. Cumulatively, the combined effect of compressor and condenser inlet air cooling increased the net power of the combined cycle power plant by 7.7%. This result is higher than that reported in previous studies [16] and [17] because these studies only considered compressor inlet air cooling but did not consider steam condenser cooling.

Furthermore, the overall thermal efficiency of the CCPP increased by 8.1% while the specific fuel consumption decreased by 7.0%. The stack discharge temperature of the exhaust flue gases after passing through the absorption refrigeration unit was determined to be 84°C.

Table 3. Comparison of power plant performance parameters with and without inlet air cooling.

Performance parameter	Gas turbine cycles	Steam turbine cycle	Combined cycle	Net change in the CCPP (%)
Net power output (MW)				
(i) Without inlet air cooling	441.3	200.0	641.3	
(ii) With compressor and condenser inlet air cooling	489.6	201.4	691.0	7.7
Thermal efficiency (%)				
(i) Without inlet air cooling	33.1	28.6	48.1	
(ii) With compressor and condenser inlet air cooling	37.1	28.8	52.0	8.1
Specific fuel consumption (kg/MWh)				
(i) Without inlet air cooling	210.8		48.3	
(ii) With compressor and condenser inlet air cooling	189.9		44.9	-7.0

The key input and computed parameters of the absorption refrigeration system are presented in Table 4. The low COP of the absorption refrigeration cycle under consideration is due to its high temperature difference between generator T_{gen} (K) and evaporator temperature, T_e (K) as may readily be verified from the equivalent Carnot COP, $(T_{gen} - T_e)/[T_{gen}(T_0 - T_e)]$.

Table 4. LiBr-H_2O absorption refrigeration system parameters.

Parameter	Value
Generator temperature, T_{gen} (°C)	95.0
Condenser temperature, T_{cond} (°C)	46.0
Absorber temperature, T_{abs} (°C)	30.0
Evaporator temperature, T_e (°C)	5.0
Input thermal energy (MW)	74.6
Total cooling load (MW)	44.4
Coefficient of performance, COP (-)	0.60

The results of the economic and environmental performance parameters of the combined cycle power plant with and without inlet air cooling of the compressor and air cooled condenser are presented in Table 5. It can be seen that by implementing inlet air cooling the total capital cost and total life cycle cost of the CCPP increased by 3.3% and 2.3%, respectively while total annual sales revenue and the net present value increased by 7.7% and 14%, respectively. Furthermore, the levelized cost of energy production in the plant and the break-even point of the investment reduced by 4.8% and 5.6%, respectively.

The environmental impact assessment revealed that the emission rates of carbon dioxide and oxides of nitrogen reduced drastically by 7.3% and 65%. This shows that the rate of CO_2 emissions per MWh from gas fired thermal power plants could be reduced by lowering the compressor inlet air temperature, as previously reported by [25]. However, it is also observed that the rate of CO emission increased with inlet air cooling in the CCPP by 12.1%. This is because the humidity of the air stream into the compressor increases with cooling. The moisture content of air may cause combustion instability resulting in increase of CO emissions and reduction in NOx emissions [64].

Table 5. Economic and environmental performance characteristic of the combined cycle plant.

Parameter	CCPP without inlet air cooling	CCPP with inlet air cooling	Net change in the CCPP (%)
Economic			
Total capital cost (MU$)	769,800,000	795,436,071	3.3
Total life cycle cost (MUS$)	1,421,236,444	1,453,664,157	2.3
Annual revenue (MUS$/yr.)	399,182,264	429,984,925	7.7
Levelized cost of energy production ($/kWh)	0.042	0.040	-4.8
Annualized life cycle cost (MUS$/yr.)	214,586,808	219,482,939	2.3
Break-even point (yr.)	3.6	3.4	-5.6
Net present value (MUS$)	1,222,599,803	1,394,178,161	14.0
Environmental			
CO_2 emission *($kgCO_2/MWh$)*	398	369	-7.3
NOx emission rate *(kg/s)*	1.70E-09	5.93E-10	-65.2
CO emission rate *(kg/s)*	1.99	2.23	12.1

3.4. Sensitivity Tests of Some Key Parameters

The influence of variations in ambient air conditions on combined cycle plant performance has been analyzed and performance curves generated by varying various parameters. Figures 4 and 5 highlight the effects of variations in ambient air temperature and relative humidity on gas turbine and combined plant performance. An increase in either temperature or relative humidity results in reduced power output within the power plant. As the density of air is inversely proportional to the temperature, the increase in air temperature results in decrease of the air density and thus lower air mass flow rate, since the volume flow rate is

constant. Consequently, the net power output decreases. These results are in agreement with previously published results [8], [17], [37].

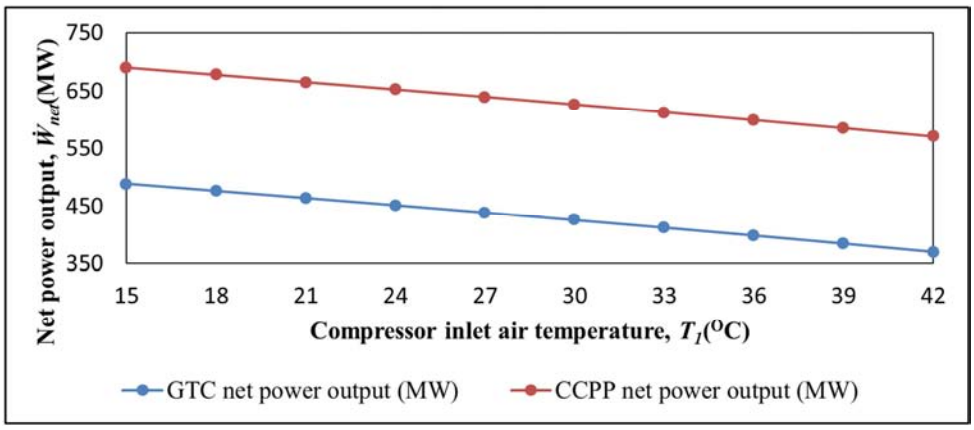

Figure 4. Effect of compressor inlet air temperature on the gas turbine-and combined cycle net power outputs.

As inlet air relative humidity increases (at constant fuel flow rate into the combustion chamber), the combustion temperature and the turbine inlet temperature decreases due to the presence of water vapor which absorbs some part of the heat of combustion [64], resulting in drop in turbine output as shown in Figure 5.

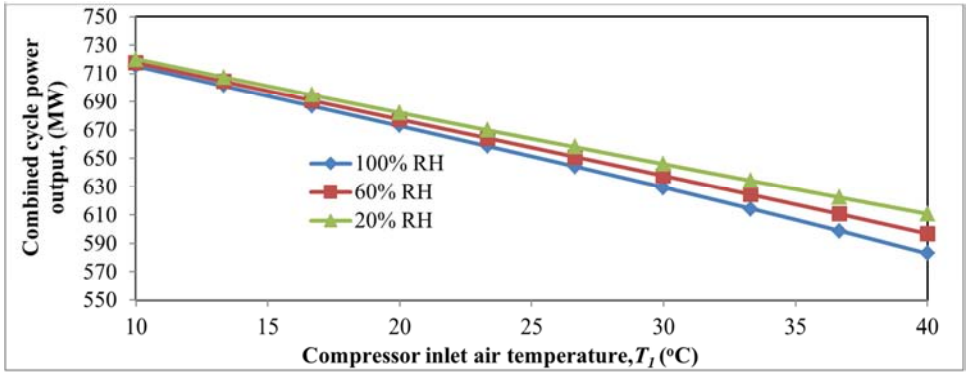

Figure 5. Effects of varying ambient temperature and relative humidity on the CCPP power output.

Figure 6 shows that, as compressor inlet air temperature increased, the thermal efficiency of the gas turbine cycle and combined cycle power plants dropped and the specific fuel consumptions increased. Similar trend was reported in reference [25].

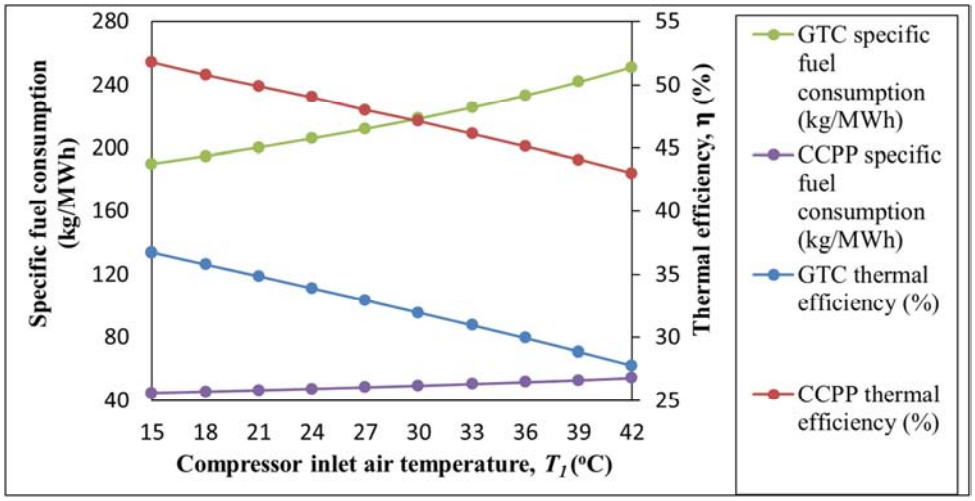

Figure 6. Variations of the gas turbine cycle and combined cycle power plant efficiencies, and specific fuel consumption, SFC (kg/MWh), with ambient inlet air temperature, T_1.

Figure 7 indicate that ambient air temperature has significant impact on the performance of an air cooled steam condenser and power output of the steam turbine cycle. As the condenser cooling air temperature increased, the steam turbine cycle power output dropped, consequently the energy efficiencies of the steam turbine cycle and combined cycle plants dropped respectively. Thus, the performances of steam turbine cycle and combined cycle power plants fitted with air cooled steam condensers, could be improved by lowering the temperature of the cooling air streams. This is in line with previous works [4], [20], [21].

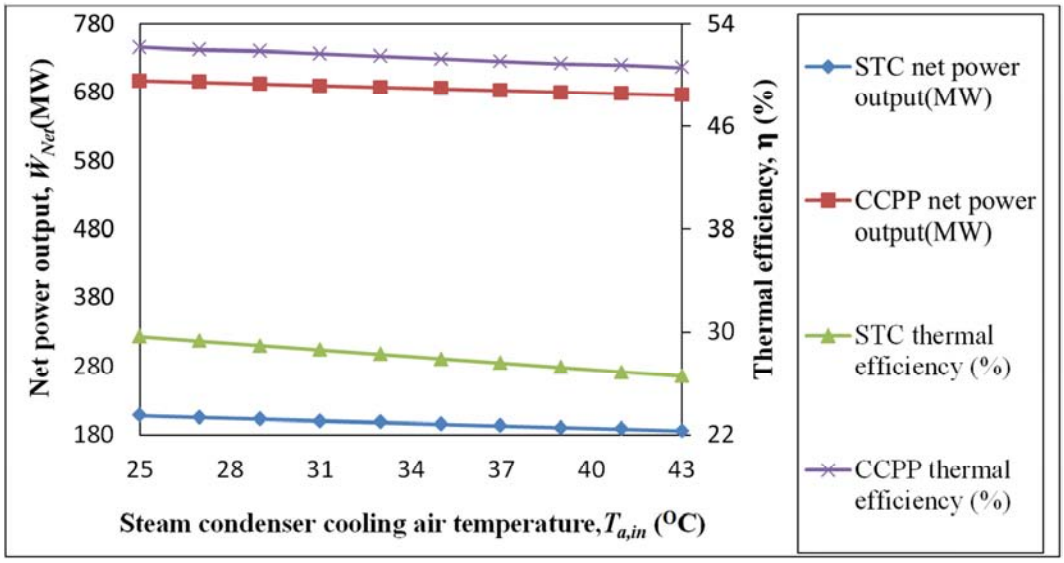

Figure 7. Steam condenser cooling air temperature versus steam turbine, combined cycle plant power output and efficiency.

The influence of some fiscal parameters such as interest rate and electricity tariff on the economic performance of combined cycle power plants, with and without inlet air cooling, was investigated. Figure 8 shows that as the interest rate in an economy is increased, the levelized cost of energy production and annualized life cycle cost of the combined cycle power plant increase. This is because the rise in interest rate affects the cost of operating and maintenance of the power plants which affects the unit cost of the plant power output. However, it can be seen that the combined cycle plant with internal cooling of inlet air streams to the compressor and steam condenser (CCPP w/cooling) has lower energy cost of production.

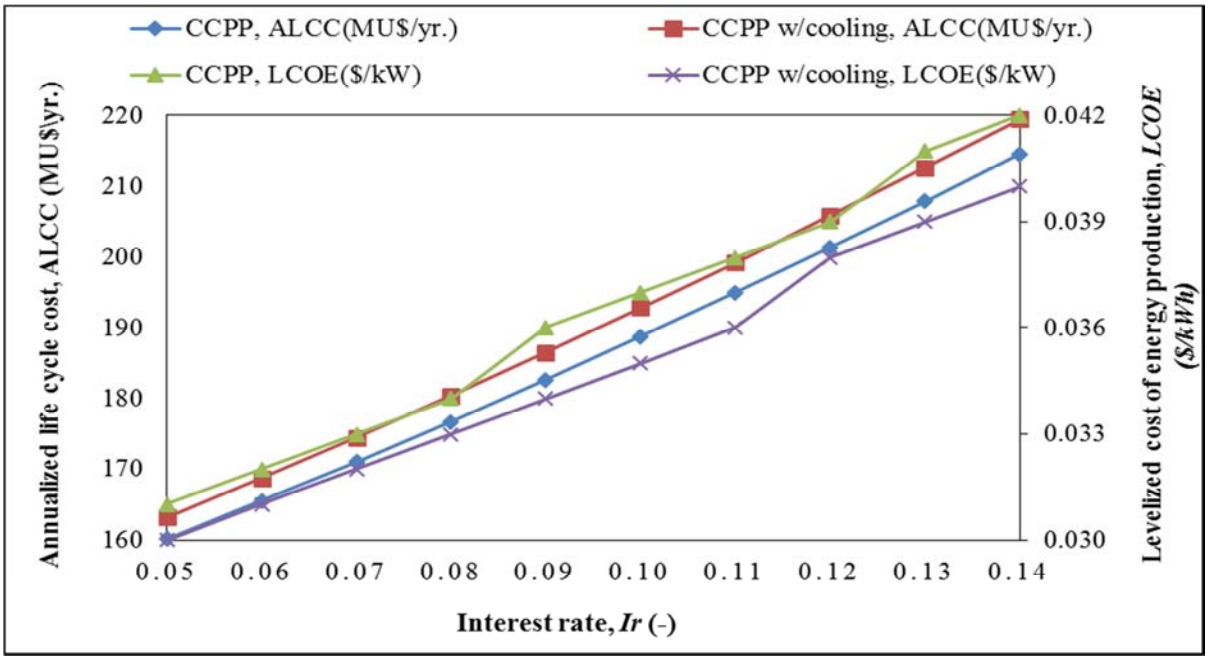

Figure 8. Effects of varying interest rates on the levelized cost of energy production and annualized life cycle cost of combined cycle power plants.

Figure 9 shows that as interest rate increase, the total life cycle cost (LCC) of the CCPP reduces and consequently, the break – even point (BEP) for the investment decrease accordingly. This is because BEP depends on LCC as can be seen from the model for computing BEP as given in reference [44]. The CCPP w/cooling has faster break-even point (return) on investment.

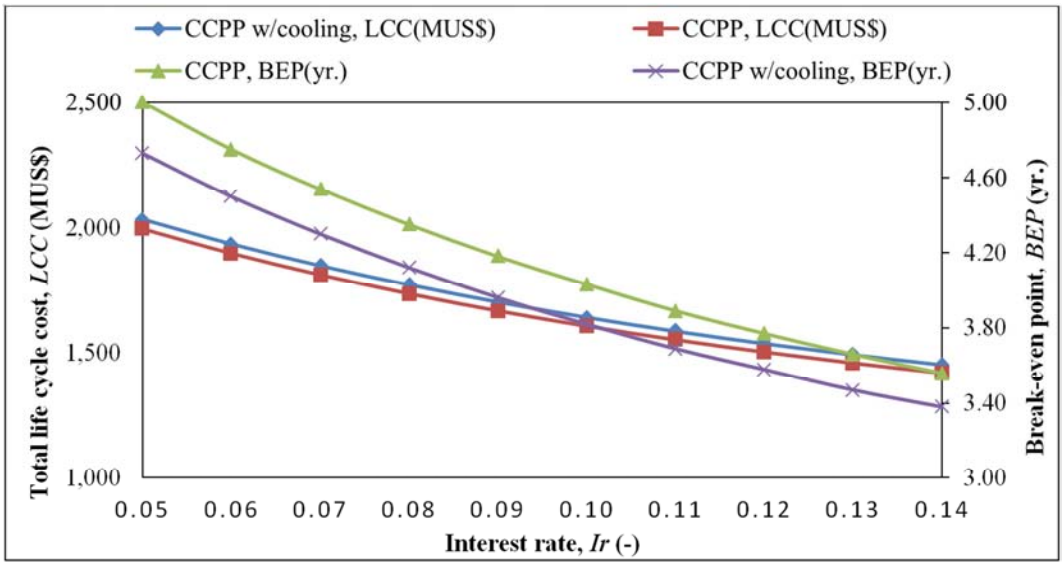

Figure 9. Total life cycle cost and break-even point as functions of the interest rate for combined cycle power plant configurations.

The impact of varying electricity tariff on the annual sales revenue from the CCPP is shown in Figure 10, it can be seen that as the electricity tariff is increased the annual revenue from the plants increased with CCPP w/cooling showing the highest annual revenue. This confirms that the electricity tariff in any location strongly affects the profitability of the power plant business.

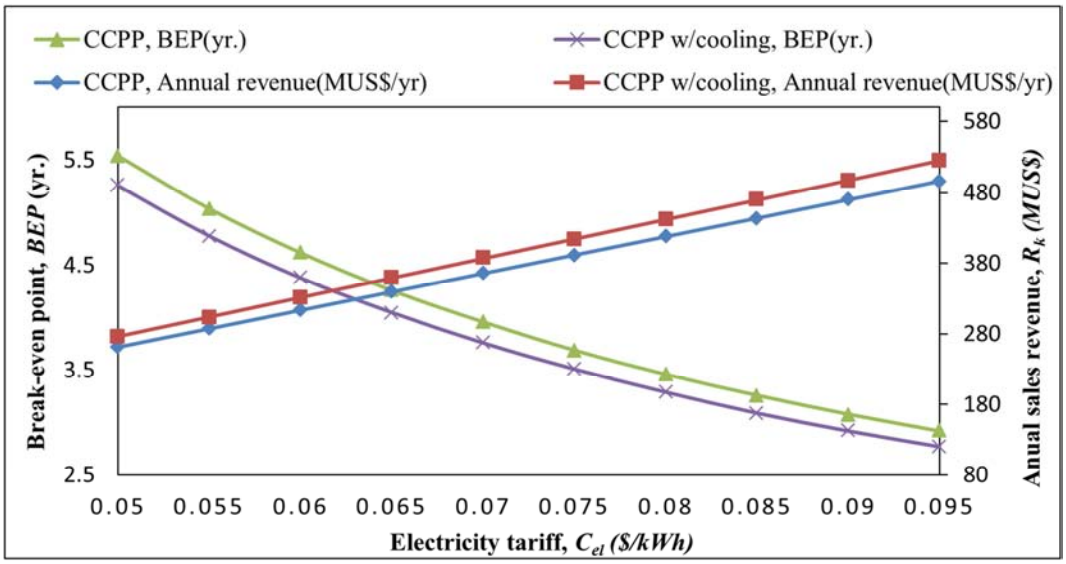

Figure 10. Dependence of the annual sales revenue on electricity tariff for combined cycle power plant configurations.

The variations of fuel mass flow rate with CO_2 emissions was also simulated for the gas turbine cycle, combined cycle plants, with and without inlet air cooling, Figure 11. The rate of CO_2 emission per megawatt-hour increased with the rate of fuel flow in the thermal power plants. This implies that the rate of CO_2 emissions could be reduced using lower fuel injection rates in the combustion chamber [26], following that the source of all carbon emissions, in fossil fuel fired power plants, is their fuels [51]. As noted earlier, it is can be observed that the combined cycle plant with inlet air cooling plant presented the lowest rate of CO_2 emissions per MWh of energy generation.

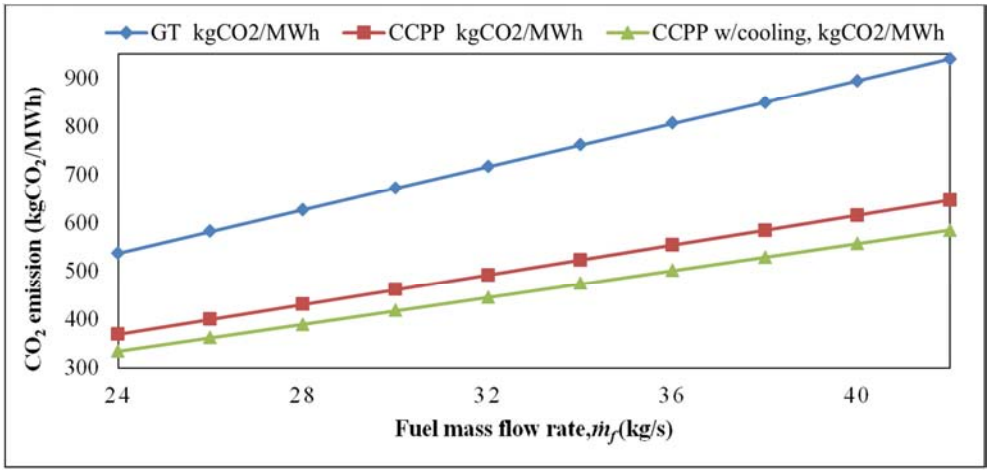

Figure 11. CO_2 emission as function of fuel mass flow rate.

Figure 12 shows the effects of combustion inlet temperature on the rates of CO and NOx emissions. The rate of NOx emission increased while CO emission decreased as the combustion inlet air temperature is reduced. This is because the higher the combustion inlet air temperature, the higher the efficiency of the combustion process in a gas turbine plant [64].

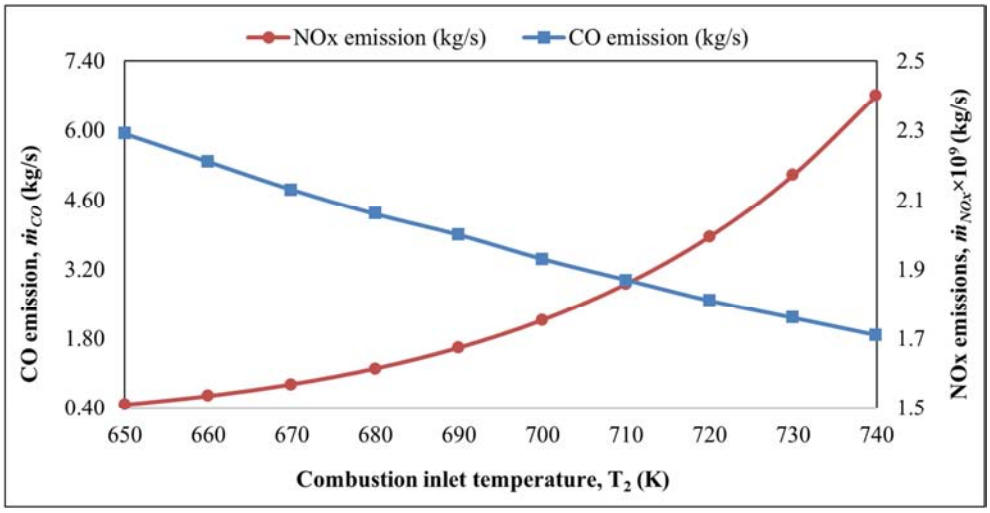

Figure 12. Effect of combustion inlet temperature (T_2) on the rates of CO and NOx emissions.

4. Conclusion

This study presents the thermodynamic, economic and environmental impact assessment of an existing combined cycle power plant retrofitted with a waste heat driven aqua lithium bromide absorption refrigerator for cooling the compressor and steam condenser inlet air streams.

Ambient air conditions substantially affect the performance of combined gas- and steam- turbine power plants operating in hot and humid regions. Previous works focused on improving the performance of the combined gas- and steam-turbine power plant by inlet air cooling of the gas turbine cycle only. However, the performance of the steam turbine cycle fitted with air cooled condenser is equally affected by varying ambient conditions which consequently impacts the overall performance of the combined cycle plant. Hence, in this study, a comparative performance assessment of combined cycle power plant, with and without inlet air cooling was conducted. The thermodynamic assessment was the based on the comparison of net power output, cycle efficiency and specific fuel consumption. The economic comparison was based on the life cycle cost, annualized life cycle cost, annual sales return, levelized cost of electricity, breakeven point and the net positive value methods. The comparative environmental impact analysis was based on the computation of the rates of CO, NOx and CO_2 emissions in kilogram per second and the rate of CO_2 per megawatt hour of energy generation, for the different CCPP configurations.

Using the operating data of an existing combined cycle power plant operating in the hot and humid tropical region of Nigeria, the results of the analysis showed that by cooling the inlet air to the compressors to 15°C, the net power output of

the gas turbine cycles increased by 48.3MW, and by cooling the inlet air streams to the air cooled steam condenser to 29°C, the net power output of the steam turbine cycle increased by 1.4MW. Cumulatively, the combined effect of compressor and condenser inlet air cooling increased the overall thermal efficiency of the CCPP by 8.1% while the specific fuel consumption decreased by 7.0%. The stack flue gas exit temperature reduced from 126°C to 84°C in the absorption refrigerator, thus reducing the exhaust heat discharge rate in to the atmosphere. The results of the economic analysis show that by implementing inlet air cooling of the compressor and condenser, the total capital cost, total life cycle cost, total annual sales revenue and the net present value of the CCPP increased by 3.3%, 2.3%, 7.7% and 14%, respectively while the levelized cost of energy production in the plant and the break-even point of the investment reduced by 4.8% and 5.6%, respectively.

The environmental impact assessment revealed that the rate of CO_2 emissions per MWh of power generation decreased by 7.3% and the emission of oxides of nitrogen (NOx) reduced drastically by 65%. However, it was also observed that the rate of CO emission increased with inlet air cooling in the CCPP by 12.1%. This is because the humidity of the air stream into the compressor increases with cooling. The moisture content of air may cause combustion instability resulting in increase of CO emissions and reduction in NOx emissions. However this effect can be overcome by installing a dehumidifier at the inlet to the combustion chamber.

Parametric investigations revealed that the net power outputs and thermal efficiencies of the gas turbine cycle (GTC), steam turbine cycle (STC) and combined cycle plant (CCPP) increased with decreasing ambient inlet air temperature. It was shown that the profitability of the investments on the combined cycle power plants depend strongly on the prevailing interest rate and electricity sale tariff at the plant location. Also, the rate of CO emissions reduced with increase in combustion inlet air temperature, whereas the NOx emissions increased.

The results of this study clearly shows, that cooling the inlet air streams to the compressor and condenser of the combined cycle power plants, operating in hot and humid locations, could lead to improved thermodynamic output and cycle efficiency, increased revenue and faster return on investment and greater environmental sustainability. It is hoped that the results will aid power plant operators in hot and humid regions seeking to make modifications for plant performance improvement.

Nomenclature

C	Capital cost, $
h	Specific enthalpy, kJ/kg
I_r	Interest rate, %
$\dot{P}$	Pumping power, kW
R_k	Annual sales revenue, $
$\dot{W}$	Power Output, MW
$\dot{W}_P$	Pumping power, kW
W_{net}	Net power output, kW
c_p	Specific heat capacity at constant pressure, kJ/kg.K
$\dot{m}$	Mass flow rate, kg/s
R	Gas constant, kJ/kg.K
s	Specific entropy, kJ/kg.K
$ALCC$	Annualized life cycle cost, $/yr.
BEP	Breakeven point, year
FOM	Fixed operating and maintenance cost, $/kW
LCC	Life cycle cost, $
$LCOE$	Levelized cost of electricity, $/kWh
N	Plant economic lifetime, year
NPV	Net present value, $
OM	Annual operating and maintenance cost, $/yr.
OPs	Annual plant operating hours, hours
P	Pressure, Pa
T	Temperature, ℃
T	Temperature, ℃ or K
$Tariff$	Unit price per kWh of electricity, $/kWh
Tpz	Adiabatic flame temperature, K
VOM	Variable operating and maintenance cost, $/MWh
Greek Letters	
β	Number of gas turbine units
Δ	Change between states
η	Efficiency
Γ	Specific heat ratio
ω	Specific humidity, kg/kg $_{da}$
ξ	Concentration by mass of LiBr in LiBr_H_2O solution

Subscripts and Superscripts

a	Air
a,v	Average
c	Compressor
cc	Combustion chamber
$cond$	Condenser
$cycle$	Thermodynamic cycle
da	Dry air
f	Fuel
g	Flue gas
gt	Gas turbine
i	Constituent or component
p	Pump
s	Steam
st	Steam turbine
t	Turbine
tot	Total
w	Water
wv	Water vapor

Abbreviations

el.Gen	Electric generator
AC	Air compressor
ACC	Air cooling coil
ARS	Absorption refrigeration system
CC	Combustion chamber
CCPP	Combined cycle power plant
COND	Condenser
GT	Gas turbine
HP	High pressure
HPFWP	High pressure feed water pump
HPST	High pressure steam turbine
HPHRSG	High pressure heat recovery steam generator
LHV	Lower heating value
LP	Low pressure
LPFWP	Low pressure feed water pump
LPHRSG	Low pressure heat recovery steam generator
LPST	Low pressure steam turbine
RH	Relative humidity
SC	Steam condenser
SH	Sensible enthalpy (or heat) change
SH_f	Sensible heat gain of fuel

References

[1] T. K. Ibrahim and M. N. Mohammed, "Thermodynamic Evaluation of the Performance of a Combined Cycle Power Plant," *Int. J. Energy Sci. Eng.*, vol. 1, no. 2, pp. 60-70, 2015.

[2] T. k Ibrahim, K. M. Mohammed, O. I. Awad, M. M. Rahman, G. Najafi, F. Basrawi, A. N. Abd Alla, and R. Mamat, "The optimum performance of the combined cycle power plant : A comprehensive review," *Renew. Sustain. Energy Rev.*, vol. 79, pp. 459-474, 2017.

[3] Z. Aminov, N. Nakagoshi, T. D. Xuan, O. Higashi, and K. Alikulov, "Evaluation of the energy efficiency of combined cycle gas turbine. Case study of Tashkent thermal power plant, Uzbekistan," *Appl. Therm. Eng.*, no. 103, pp. 501-509, 2016.

[4] C. Chuang and D. Sue, "Performance effects of combined cycle power plant with variable condenser pressure and loading," *Energy*, vol. 30, pp. 1793-1801, 2005.

[5] J. G. Bustamante, A. S. Rattner, and S. Garimella, "Achieving near-water-cooled power plant performance with air-cooled condensers," *Appl. Therm. Eng.*, pp. 1-10, 2015.

[6] A. M. Al-ibrahim and A. Varnham, "A review of inlet air-cooling technologies for enhancing the performance of combustion turbines in Saudi Arabia," *Appl. Therm. Eng.*, vol. 30, no. 14-15, pp. 1879-1888, 2010.

[7] G. M. Zaki, R. K. Jassim, and M. M. Alhazmy, "Energy, Exergy and Thermoeconomics Analysis of Water Chiller Cooler for Gas Turbines Intake Air Cooling," *Smart Grid Renew. Energy*, vol. 2, pp. 190-205, 2011.

[8] R. Hosseini, A. Beshkani, and M. Soltani, "Performance improvement of gas turbines of Fars (Iran) combined cycle power plant by intake air cooling using a media evaporative cooler," *Energy Convers. Manag.*, vol. 48, pp. 1055-1064, 2007.

[9] O. K. Singh, "Performance enhancement of combined cycle power plant using inlet air cooling by exhaust heat operated ammonia-water absorption refrigeration system," *Appl. Energy*, vol. 180, pp. 867-879, 2016.

[10] M. Ameri and S... Hejazi, "The study of capacity enhancement of the Chabahar gas turbine installation using an absorption chiller," *Appl. Therm. Eng.*, vol. 24, pp. 59-68, 2004.

[11] M. A. Ehyaei, M. Tahani, P. Ahmadi, and M. Esfandiari, "Optimization of fog inlet air cooling system for combined cycle power plants using genetic algorithm," *Appl. Therm. Eng.*, no. 76, pp. 449-461, 2015.

[12] B. Dawoud, Y. H. Zurigat, and J. Bortmany, "Thermodynamic assessment of power requirements and impact of different gas-turbine inlet air cooling techniques at two different locations in Oman of different gas-turbine inlet air cooling techniques at two," *Appl. Therm. Eng.*, vol. 25, pp. 1579-1598, 2005.

[13] G. Barigozzi, A. Perdichizzi, C. Gritti, and I. Guaiatelli, "Techno-economic analysis of gas turbine inlet air cooling for combined cycle power plant for different climatic conditions," *Appl. Therm. Eng.*, vol. 82, pp. 57-67, 2015.

[14] Y. S. H. Najjar and A. Abubaker, "Indirect Evaporative Combined Inlet Air Cooling With Gas Turbines as a Greening Technology," *Int. J. Refrig.*, vol. 59, no. 2015, pp. 235-250, 2015.

[15] M. M. Alhazmy and Y. S. H. Najjar, "Augmentation of gas turbine performance using air coolers," *Appl. Therm. Eng.*, vol. 24, pp. 415-429, 2004.

[16] S. Boonnasa, P. Namprakai, and T. Muangnapoh, "Performance improvement of the combined cycle power plant by intake air cooling using an absorption chiller," *Energy*, vol. 31, no. 12, pp. 1700-1710, 2006.

[17] A. K. Mohapatra, "Thermodynamic assessment of impact of inlet air cooling techniques on gas turbine and combined cycle performance," *Energy*, no. 68, pp. 191-203, 2014.

[18] L. Yang, H. Tan, X. Du, and Y. Yang, "Thermal- flow characteristics of the new wave- finned flat tube bundles in air-cooled condensers," *Int. J. Therm. Sci.*, vol. 53, pp. 166-174, 2012.

[19] A. R. V Ramani, B. A. Paul, and D. A. D. Saparia, "Performance Characteristics of an Air-Cooled Condenser Under Ambient Conditions," in *International Conference on Current Trends in Technology 'NUiCONE – 2011*, 2011, pp. 382-481.

[20] V. Gadhamshetty, N. Nirmalakhandan, M. Myint, and C. Ricketts, "Improving Air-Cooled Condenser Performance in Combined Cycle Power Plants," *J. Eng. Energy*, vol. 132, no. 2, pp. 81-88, 2006.

[21] N. Nirmalakhandan, V. Gadhamshetty, and A. Mummaneni, "Improving Combined Cycle Power Plant Performance," in *6th International Conference on Heat Transfer, Fluid Mechanics and Thermodynamics*, 2008, no. MN1, pp. 1-6.

[22] A. Ataei, M. H. Panjeshahi, and M. Gharaie, "Performance evaluation of counter-flow wet cooling towers using exergetic analysis," *Trans. CSME/de la SCGM*, vol. 32, no. 3-4, pp. 499-512, 2008.

[23] C. O. C. Oko and O. B. Ogoloma, "Generation of a typical meteorological year," *J. Eng. Sci. Technol.*, vol. 6, no. 2, pp. 204-214, 2011.

[24] S. O. Oyedepo, R. O. Fagbenle, S. S. Adefila, and M. Alam, "Thermoeconomic and thermoenvironomic modeling and analysis of selected gas turbine power plants in Nigeria," *Energy Sci. Eng.*, vol. 3, no. 5, pp. 423-442, 2015.

[25] A. G. Memon, K. Harijan, M. A. Uqaili, and R. A. Memon, "Thermo-environmental and economic analysis of simple and regenerative gas turbine cycles with regression modeling and optimization," *Energy Convers. Manag.*, vol. 76, pp. 852-864, 2013.

[26] P. Ahmadi, I. Dincer, and M. A. Rosen, "Exergy, exergoeconomic and environmental analyses and evolutionary algorithm based multi-objective optimization of combined cycle power plants," *Energy*, vol. 36, pp. 5886-5898, 2011.

[27] P. K. Nag, *Power Plant Engineering*, 3rd ed. New Delhi: Tata McGraw Hill Education, 2013.

[28] A. K. Tiwari, M. M. Hasan, and M. Islam, "Exergy Analysis of Combined Cycle Power Plant : NTPC Dadri, India," *Int. J. Thermodyn.*, vol. 16, no. 1, pp. 36-42, 2013.

[29] T. K. Ibrahim and M. M. Rahman, "Effect of Compression Ratio on Performance of Combined Cycle Gas Turbine," *Int. J. Energy Eng.*, vol. 2, no. 1, pp. 9-14, 2012.

[30] M. T. Mansouri, P. Ahmadi, A. Ganjeh, and M. N. M. Jaafar, "Exergetic and economic evaluation of the effect of HRSG configurations on the performance of combined cycle power plants," *Energy Convers. Manag.*, vol. 58, pp. 47-58, 2012.

[31] P. Ahmadi and I. Dincer, "Thermodynamic analysis and thermoeconomic optimization of a dual pressure combined cycle power plant with a supplementary firing unit," *Energy Convers. Manag.*, vol. 52, no. 5, pp. 2296-2308, 2011.

[32] A. G. Kaviri, M. N. M. Jaafar, and T. M. Lazim, "Modeling and multi-objective exergy based optimization of a combined cycle power plant using a genetic algorithm," *Energy Convers. Manag.*, vol. 58, pp. 94-103, 2012.

[33] Y.. Cengel and M. A. Boles, *Thermodynamics: An Engineering Approach*, 7th ed. New York: McGraw-Hill Publishing Company, 2011.

[34] A. O. Donovan and R. Grimes, "A theoretical and experimental investigation into the thermodynamic performance of a 50 MW power plant with a novel modular air-cooled condenser," *Appl. Therm. Eng.*, vol. 71, no. 1, pp. 119-129, 2014.

[35] I. Dinçer, M. Rosen, and P. Ahmadi, *Optimization of Energy Systems*. UK: Wiley, 2018.

[36] I. Dincer and T. Ratlamwala, *Integrated Absorption Refrigeration Systems*. Switzerland: Springer, 2016.

[37] S. Popli, P. Rodgers, and V. Eveloy, "Gas turbine efficiency enhancement using waste heat powered absorption chillers in the oil and gas industry," *Appl. Therm. Eng.*, vol. 50, no. 1, pp. 918-931, 2013.

[38] R. Touaibi, M. Feidt, E. E. Vasilescu, and M. Tahar Abbes, "Parametric study and exergy analysis of solar water- lithium bromide absorption cooling system," *Int. J. Exergy*, vol. x, no. x, pp. 1-16, 2013.

[39] S. C. Kaushik and A. Arora, "Energy and exergy analysis of single effect and series flow double effect water – lithium bromide absorption refrigeration systems," *Int. J. Refrig.*, vol. 32, no. 6, pp. 1247-1258, 2009.

[40] K. Muhsin and O. Kaynakli, "Second law-based thermodynamic analysis of water-lithium bromide absorption refrigeration system," *Energy*, vol. 32, pp. 1505-1512, 2007.

[41] C. O. C. Oko and E. O. Diemuodeke, "Analysis of air-conditioning and drying processes using spreadsheet add-in for psychrometric data," *J. Eng. Sci. Technol. Rev.*, vol. 3, no. 1, pp. 7-13, 2010.

[42] V. L. Le, A. Kheiri, M. Feidt, and S. Pelloux-prayer, "Thermodynamic and economic optimizations of a waste heat to power plant driven by a subcritical ORC (Organic Rankine Cycle) using pure or zeotropic working fluid," *Energy*, vol. 78, pp. 622-638, 2014.

[43] G.. Tiwari and R.. Mishra, *Advanced Renewable Energy Sources*. Cambridge: RSC Publishing, 2012.

[44] C. O. C. Oko, E. O. Diemuodeke, N. F. Omunakwe, and E. Nnamdi, "Design and Economic Analysis of a Photovoltaic System : A Case Study," *Int. J. Renew. Energy Dev.*, vol. 1, no. 3, pp. 65-73, 2012.

[45] B. Tchanche, S. Quoilin, S. Declaye, G. Papadakis, and V. Lemort, "Economic Feasibility Study of a Small Scale Organic Rankine Cycle System in Waste Heat Recovery Application," in *Proceedings of the ASME 2010 10th Biennial Conference on Engineering Systems Design and Analysis ESDA 2010*, 2010, no. July 12-14, pp. 1-9.

[46] D. Walraven, B. Laenen, and W. D'haeseleer, "Economic system optimization of air-cooled organic Rankine cycles powered by low- temperature geothermal heat sources," *Energy*, vol. 80, pp. 104-113, 2015.

[47] N. K. Rizk and H. C. Mongia, "Semianalytical Correlations for NOx, CO, and UHC Emissions," *Am. Soc. Mech. Eng.*, vol. 92, pp. 1-8, 1992.

[48] A. Ã. Lazzaretto and A. Toffolo, "Energy, economy and environment as objectives in multi-criterion optimization of thermal systems design," *Energy*, vol. 29, pp. 1139-1157, 2004.

[49] P. Ahmadi and I. Dincer, "Thermodynamic and exergoenvironmental analyses, and multi-objective optimization of a gas turbine power plant," *Appl. Therm. Eng.*, vol. 31, no. 14–15, pp. 2529-2540, 2011.

[50] M. A. Ehyaei, S. Hakimzadeh, N. Enadi, and P. Ahmadi, "Exergy, economic and environment (3E) analysis of absorption chiller inlet air cooler used in gas turbine power plants," *Int. J. energy Res.*, vol. 36, pp. 486-498, 2012.

[51] A. Ganjehkaviri, M. N. M. Jaafar, P. Ahmadi, and H. Barzegaravval, "Modelling and optimization of combined cycle power plant based on exergoeconomic and environmental analyses," *Appl. Therm. Eng.*, vol. 67, no. 1-2, pp. 566-578, 2014.

[52] A. Ganjehkaviri, M. N. M. Jaafar, and S. E. Hosseini, "Optimization and the effect of steam turbine outlet quality on the output power of a combined cycle power plant," *Energy Convers. Manag.*, vol. 89, pp. 231-243, 2015.

[53] P. Ahmadi, I. Dincer, and M. A. Rosen, "Thermodynamic modeling and multi-objective evolutionary-based optimization of a new multigeneration energy system," *Energy Convers. Manag. J.*, vol. 76, pp. 282-300, 2013.

[54] Afam VI Combined Cycle Gas Turbine Plant (CCGT), "Plant operations report," Afam, Nigeria, 2015.

[55] H. I.. Saravanamuttoo, H. Cohen, and G. F.. Rogers, *Gas Turbine Theory*, 4th ed. London: Longman, 1996.

[56] WECC, "Capital Cost Review of Power Generation Technologies: Recommendations for WECC's 10- and 20-Year Studies," Salt Lake City, 2014.

[57] U.S. Energy Information Administration, "Updated Capital Cost Estimates for Utility Scale Electricity Generating Plants," Washington DC, 2013.

[58] Energy Innovators Initiative, "Choosing a High-Efficiency Chiller System," Ottawa, 2009.

[59] G. Mohan, S. Dahal, U. Kumar, A. Martin, and H. Kayal, "Development of Natural Gas Fired Combined Cycle Plant for Tri-Generation of Power, Cooling and Clean Water Using Waste Heat Recovery: Techno-Economic Analysis," *energies*, vol. 7, pp. 6358-6381, 2014.

[60] Trading Economics, "Nigeria Interest Rate 2007-2016 | Data | Chart | Calendar | Forecast," *Accessed 11-08-2016*, 2016.

[61] J. Kotowicz, M. Job, and M. Brze, "The characteristics of ultramodern combined cycle power plants," *Energy*, pp. 1-15, 2015.

[62] District Energy, "Cooling service rates 2016," *District Energy St. Paul*, 2016..

[63] CSL Stockbrokers, "Nigerian Power Sector," London, 2014.

[64] M. Jonsson and J. Yan, "Humidified gas turbines — a review of proposed and implemented cycles," *Energy*, vol. 30, pp. 1013-1078, 2005.